MESH DEFORMATION WITH EXACT SURFACE RECONSTRUCTION USING A REDUCED RADIAL BASIS FUNCTION APPROACH

DANIEL S. C. KOWOLLIK, MATTHIAS C. HAUPT AND PETER HORST

Institute of Aircraft Design and Lightweight Structures (IFL)
TU Braunschweig
Herrmann-Blenk-Str. 35, 38106 Braunschweig, Germany
e-mail: d.kowollik@tu-braunschweig.de, web page: http://www.tu-braunschweig.de/ifl

Key words: Mesh deformation, Mesh motion, Radial basis functions, Delaunay graph mapping, Fluidstructure interaction

Abstract. This paper presents a novel reduced radial basis function approach with exact surface reconstruction. The new approach combines two well proven mesh deformation algorithms in a three step approach. In a first pre-processing step an explicit reduction of radial basis function points is performed using a k-d tree. In the second step the classic radial basis function interpolation is used to propagate the deformation field. In a last post-processing step an exact surface reconstruction is achieved using an efficient Delaunay graph mapping approach. The new mesh deformation approach is compared to the two original approaches by investigating a 2D viscous mesh test case. The applicability of the new approach to 3D is shown via an aeroelastic relevant wing test case.

1 INTRODUCTION

The demand of mesh deformation algorithms for computational fluid dynamic (CFD) meshes arises for instance in shape optimization analyses or in fluid-structure interaction (FSI) analyses. During FSI analyses for each iteration and time step a CFD mesh deformation is required in order to follow the structural response. The interest for more detailed analyses and complex configurations in the aeronautical industry such as the analyses of complete aircrafts including slats, pylons and flaps increase the computational cost substantially for each involved algorithm. A transient FSI analysis may require several hundred of mesh deformations. Therefore, a robust and efficient technique is required.

The published algorithms can be categorized into two groups, the once that are point schemes and the once that are connectivity schemes.

Connectivity Schemes are mainly dominated by structural analogy approaches. Either the edges of the cells or the cells directly are treated as a mechanical model such as springs

or plates. A structural finite element model can be formulated and a linear sparse system needs to be solved. A classic approach is the spring analogy presented by Batina [1], which treats the cell edges as linear springs, where the stiffness of the springs is computed by the inverse of the individual edge length. This approach can lead to degenerated cells if one pair of edges snaps through the other edges of the same cell. To minimise this problem Farhat et al. [2] developed the torsional spring method. In addition to the classic approach torsional springs are added to the corners of the cells to prevent the cells from colliding. Continuum elastic approaches have been suggested by Lynch et al. [3] and improved by Stein et al. [4]. The common feature of these approaches is an increasing stiffness with decreasing cell size. This may result in a stiff system matrix which often allows only small incremental deformations. Furthermore, these methods are difficult to implement for arbitrary mesh types especially for meshes with hanging nodes.

Point schemes directly support arbitrary mesh types because an interpolation algorithm is used which propagates the boundary movements without taking the mesh connectivity into account. An efficient algorithm developed by Liu et al. [10] is based on a coarse Delaunay mesh which is generated using the boundary and far field points. The deformations are propagated with the Delaunay graph through a linear mapping using barycentric coordinates. The drawback of this approach is a strong shearing of orthogonal aligned cells near the boundary if large deformations are present. Mesh deformation based on radial basis functions (RBFs) has been studied by several authors [5, 6, 7, 8] and has shown to generate smooth mesh deformations. If an appropriate RBF is used, a good orthogonal behaviour near the structured boundary layer is achieved. The drawback of the original form of the RBF approach is the large linear dense system that needs to be solved if a large amount of source deformation points is present. RBFs with compact support presented by Wendland [9] allow the reduction of the system to a sparse one. If the radius is small, only small deformations can be incorporated inside the volume mesh which limits this reduction technique. Consequently, RBF mesh deformation is only applicable to large meshes if a reduction of source points is performed. This reduction results in an inexact surface deformation which might lead to unsatisfactory results if too many source points are eliminated. In order to minimise this effect Rendall et al. [8] proposed different Greedy algorithms to make an optimal choice of a source point reduction. Subsequent to the RBF deformation a correction function is used to account for the dropped surface points. The method is more efficient compared to the classic RBF deformation and generates good results, however during a transient FSI analysis the optimization problem has to be solved at least once if the deformations are small or more often if the deformation variation is large. In this paper we present an alternative explicit reduced RBF deformation approach with exact surface reconstruction based on the Delaunay graph mapping (DGM) approach developed by Liu et. al [10]. In the following we present the numerical approach and use a 2D aeroelastic relevant test case to analyse and discuss the quality of the new algorithm compared to the original RBF and DGM approach. Last, we demonstrate the applicability of the new approach to a 3D wing test case.

2 NUMERICAL APPROACH

Our hybrid approach combines two well proven mesh deformation techniques in a three-step approach:

I. The first pre-processing step is needed to perform a reduction of deformation source points in order to achieve a small limited amount of source points for the following RBF deformation step. Different methods are possible to reduce the number of source points. In this study we suggest an explicit reduction technique using a k-d tree. A reduced number of source points are extracted from each leaf to determine a good representation of the provided source points.

II. The second RBF deformation step uses the reduced number of source points to induce the reduced deformation field to the volume mesh points, which results in an inexact surface deformation.

III. In a third post-processing step a remaining offset deformation vector between the initial surface deformation and the resulting reduced RBF deformation is computed. This offset vector is propagated to the volume mesh points by using the DGM approach in order to reconstruct the exact surface.

2.1 Source point reduction technique

An explicit source point reduction technique is developed, which is not connected to the current deformation field. The advantage of this approach is a so called black box method, which can be applied to the initial undeformed mesh at the beginning of an FSI analyses. The information of the reduced number of source points can be stored and reused in each deformation step.

A lot of different approaches are possible. For instance, one could use the connectivity of the boundary mesh and use the generated multigrid meshes of the CFD analyses code. We suggest a point based approach based on a k-d tree. This approach holds on to the requirement that an entire point based approach is desired, which makes the overall approach suitable to a more generic application field.

The present k-d tree is generated using the open source library vtk [13], which allows a broad direct access to the generated k-d tree data structure. The k-d tree algorithm is not used in the original sense that the access time and search time to locate a point is optimized. Moreover, we use the control parameters of the division of spatial block regions in order to generate as many leaf regions as desired. A small region is generated where a local clustering of surface points is located, e.g. the leading edge of a wing or a shock position on the surface. The bounding box of each leaf region is used to construct search points inside the region. These search points are only used to find a close source point (surface point) and therefore generate an explicit generated limited number of source points for the subsequent RBF deformation step.

The source point reduction technique can be subdivided in the following steps:

1. Construction of a k-d tree with minimal and maximal allowable region bounds.

2. Gather the bounding boxes of each generated leaf region.

3. Generate search points for each region using linear hexahedron finite elements.

4. Find the closest mesh point to each search point.

5. Drop the duplicate found mesh points.

The position of generated search points inside each region can be arbitrary as desired. So far we used 1 central point, 8 gauss points ($\pm 1/\sqrt{3}$, $\pm 1/\sqrt{3}$, $\pm 1/\sqrt{3}$) or 8 corner points depending on the test case.

Two different generated coarse k-d trees are shown in figure 1. In figure 1(a) one can see the used search points in red (corner points) and the found mesh points in green of the entire boundary mesh point set (yellow triangles). Figure 1(b) shows a coarse k-d tree generated for the 3D wing test case. A finer k-d tree would consequently generate more leaf regions along the leading and trailing edge of the wing.
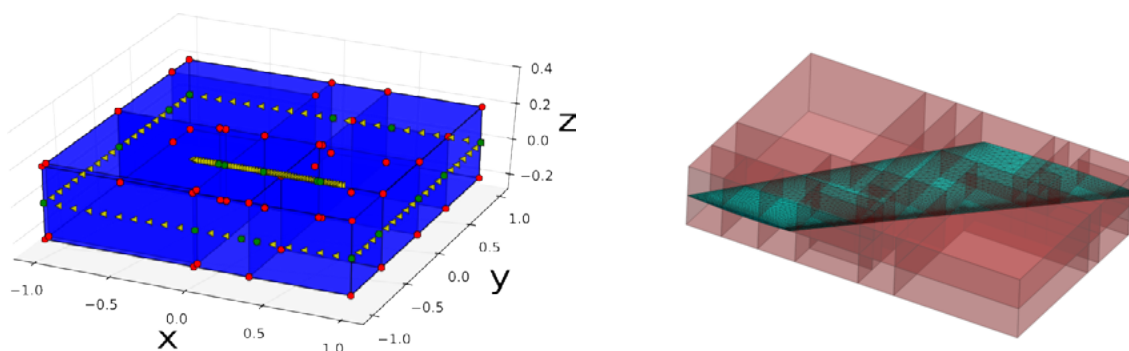
(a) k-d tree (blue) applied to a simple test case; mesh points (yellow); k-d tree search points (red); reduced RBF points (green).

(b) k-d tree (red) applied to the surface of the wing test case.

Figure 1: Illustrations of the coarse k-d tree representation used for the source point reduction).

2.2 Radial basis function interpolation

RBF based mesh deformation is a point based interpolation approach which propagates the displacement field $\mathbf{u}_j^s$ of a finite set of source points $\mathbf{x}_j^s = \left[x_{1j}^s, x_{2j}^s, x_{3j}^s \right]$, $j = 1, 2, ..., n_s$ using a continuous interpolation function $c(\mathbf{x}_i^t)$:

$$c(\mathbf{x}) = p(\mathbf{x}) + \sum_j^{n_s} \beta_j \, \phi \left(\| \mathbf{x} - \mathbf{x}_j^s \| \right) \ . \tag{1}$$

A smooth interpolation is realized by a linear combination of basis functions ϕ being radial with respect to the Euclidean distance of the source points. For an exact recovery of rigid body motions a linear polynomial $p(\mathbf{x}) = \alpha_0 + \alpha_1 x_1 + \alpha_2 x_2 + \alpha_3 x_3$ is added in the case of RBF based mesh deformation. The inclusion of the linear polynomial requires the fulfilment of an additional zero condition:

$$\sum_{j}^{n_s} \beta_j q\left(\mathbf{x}_j^s\right) = 0 \;, \tag{2}$$

for all polynomials q with degree $\deg(q) \leq \deg(p)$. The weights of the linear polynomial α_i and the RBF's β_j can be evaluated by solving the linear system

$$\begin{bmatrix} 0 \\ 0 \\ 0 \\ 0 \\ c_1^s \\ c_2^s \\ \vdots \\ c_{n_s}^s \end{bmatrix} = \begin{bmatrix} 0 & 0 & 0 & 0 & 1 & 1 & \cdots & 1 \\ 0 & 0 & 0 & 0 & x_{1,1}^s & x_{1,2}^s & \cdots & x_{1,n_s}^s \\ 0 & 0 & 0 & 0 & x_{2,1}^s & x_{2,2}^s & \cdots & x_{2,n_s}^s \\ 0 & 0 & 0 & 0 & x_{3,1}^s & x_{3,2}^s & \cdots & x_{3,n_s}^s \\ 1 & x_{1,1}^s & x_{2,1}^s & x_{3,1}^s & \phi_{1,1}^s & \phi_{1,2}^s & \cdots & \phi_{1,n_s}^s \\ 1 & x_{1,2}^s & x_{2,2}^s & x_{3,2}^s & \phi_{2,1}^s & \phi_{2,2}^s & \cdots & \phi_{2,n_s}^s \\ \vdots & \vdots & \vdots & \vdots & \vdots & \vdots & \vdots & \vdots \\ 1 & x_{1,n_s}^s & x_{2,n_s}^s & x_{3,n_s}^s & \phi_{n_s,1}^s & \phi_{n_s,2}^s & \cdots & \phi_{n_s,n_s}^s \end{bmatrix} \begin{bmatrix} \alpha_0 \\ \alpha_1 \\ \alpha_2 \\ \alpha_3 \\ \beta_1 \\ \beta_2 \\ \vdots \\ \beta_{n_s} \end{bmatrix} \tag{3}$$

or in matrix form $\mathbf{c} = \mathbf{A}\mathbf{w}$ with the symmetric interpolation matrix $\mathbf{A}$. The RBF's $\phi_{ij} = \phi\left(\|\mathbf{x}_i^s - \mathbf{x}_j^s\|\right)$ in (3) are evaluated for the Euclidean distance of the source points. The formulation of the linear system (3) holds for a scalar displacement field. The extension to two or three dimensions is a trivial task. Therefore, $3 \times n_s$ weights have to be evaluated for a 3D mesh deformation. In the case of global RBF's a dense system $(4+n_s) \times (4+n_s)$ needs to be solved. Wendland introduced in [11] compact RBF's where sparsity of the system is controlled via a compact support radius. Smaller support radii generate a system which can be solved more efficiently. However, this counteracts towards an accuracy decrease of the deformation algorithm. Another drawback of small radii is a decrease of maximal allowable deformations in one deformation step. For the original version of the deformation approach the entire boundary points are used as source points. Therefore, the original form of the RBF based mesh deformation algorithm is only practical for a small number of source points.

The evaluated interpolation weights α_i and β_j can be used in the same linear combination to compute the deformation of the target points $\mathbf{x}_i^t = \left[x_{1i}^t, x_{2i}^t, x_{3i}^t\right], i = 1, 2, ..., n_t$:

$$c(\mathbf{x}_i^t) = p(\mathbf{x}_i^t) + \sum_{j}^{n_s} \beta_j \phi\left(\|\mathbf{x}_i^t - \mathbf{x}_j^s\|\right) \;. \tag{4}$$

For a more detailed study and discussion on the original form of the deformation approach and the appropriate choice of RBF types we refer to [5, 6]. One can determine from their

studies that the performance of the mesh deformation algorithm depends highly on the chosen RBF.

Using an appropriate reduction technique one can limit the number of source points which limits in equal measure the numerical cost to solve the linear system.

In [6] it was shown that the final deformed mesh can be improved if a large deformation field is subdivided into multiple incremental steps. Therefore, one can conclude that the deformation algorithm is path dependant if more than one step is used for an FSI analyses.

2.3   Surface reconstruction based on Delaunay Graph Mapping

The surface reconstruction technique suggested in this paper can be seen as an additional post-processing mesh deformation step. Large deformations are propagated with a limited number of source points using the presented RBF algorithm. A limited number of source points results in an inexact surface deformation which leads to an accuracy decrease of the overall CFD analyses. In order to eliminate this effect an exact surface reconstruction is desired. One can consider the surface reconstruction as an additional mesh deformation step based on small deformations that have to be propagated inside the volume part of the mesh. We suggest the application of the DGM algorithm proposed by Liu et al. [10], which is a very efficient point based scheme. The remaining deformation to reconstruct the exact moving boundary can be easily evaluated:

$$\mathbf{u}^b_{DGM} = \mathbf{u}^b - \mathbf{u}^b_{RBF} \tag{5}$$

The DGM mesh deformation algorithm can be divided into four steps:

1. Construction of a Delaunay graph using all boundary points.

2. Locating the volume mesh points inside the Delaunay graph.

3. Prescribing the deformation field to the Delaunay graph.

4. Relocate the volume mesh points inside the deformed Delaunay graph.

A graphical representation of the four necessary sub-steps is given for a simple test case in figure 2. If in step 3 a negative area in 2D or a negative volume in 3D is created for one of the Delaunay cells one can subdivide the deformation field and reiterate the steps one till four until the entire deformation field is propagated. However, in general this is only the case if large deformations are to be propagated with this algorithm.

Several efficient open source libraries exist which allow the construction of a Delaunay graph. For the present study we use the qhull library developed by Barber et al. [12]. A unique linear mapping of the boundary points exists for the constructed coarse mesh. In terms of barycentric coordinates the linear mapping between a field point $\mathbf{x}_P$ and the cell corner points $\mathbf{x}_A$, $\mathbf{x}_B$ and $\mathbf{x}_C$ is evaluated by:

| undeformed mesh | step 1 | step 2 |
| step 3 | step 4 | deformed mesh |
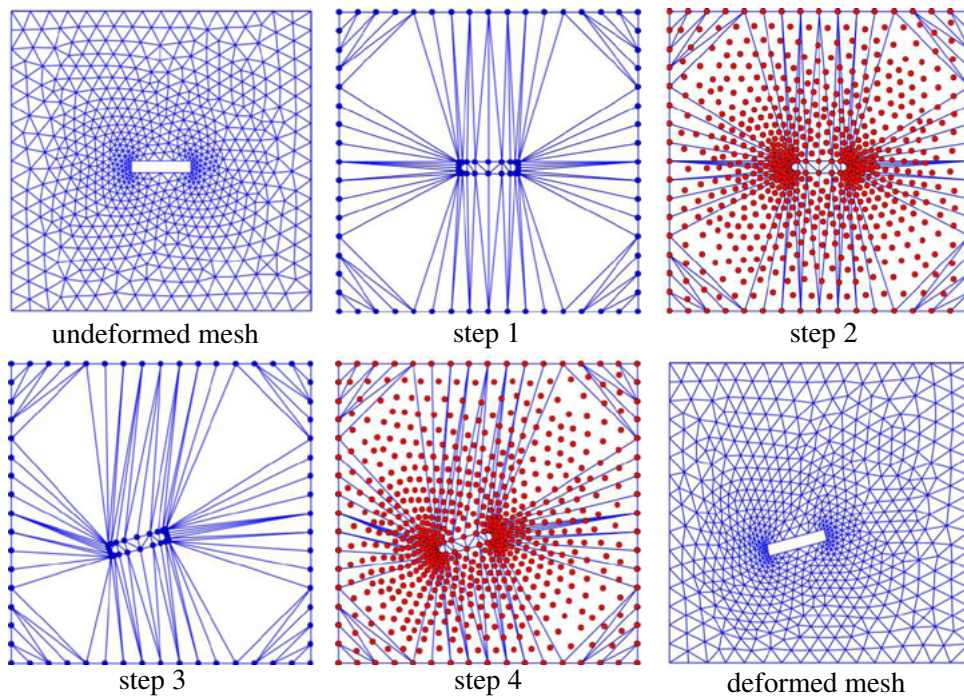
Figure 2: Sub-steps of the DGM mesh deformation algorithm.

$$\mathbf{x}_P = e_1 \cdot \mathbf{x}_A + e_2 \cdot \mathbf{x}_B + e_3 \cdot \mathbf{x}_C \qquad \text{with} \qquad e_i = \frac{S_i}{S} \ , \tag{6}$$

where e_i are the area ratio coefficients which are illustrated in figure 3 and can be determined using the partial areas S_i as follows:
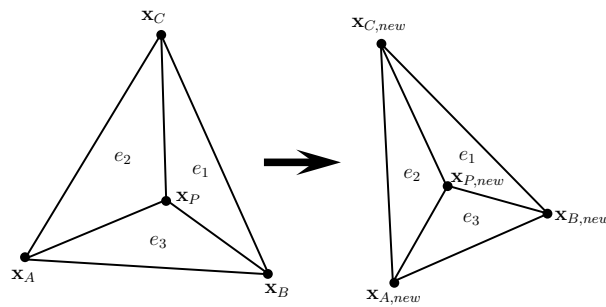
Figure 3: Linear mapping using barycentric coordinates.

$$S_1 = \frac{1}{2}\begin{vmatrix} x_{1,P} & x_{2,P} & 1 \\ x_{1,B} & x_{2,B} & 1 \\ x_{1,C} & x_{2,C} & 1 \end{vmatrix} \qquad S_2 = \frac{1}{2}\begin{vmatrix} x_{1,A} & x_{2,A} & 1 \\ x_{1,P} & x_{2,P} & 1 \\ x_{1,C} & x_{2,C} & 1 \end{vmatrix}$$

$$S_3 = \frac{1}{2}\begin{vmatrix} x_{1,A} & x_{2,A} & 1 \\ x_{1,B} & x_{2,B} & 1 \\ x_{1,P} & x_{2,P} & 1 \end{vmatrix} \qquad S = \frac{1}{2}\begin{vmatrix} x_{1,A} & x_{2,A} & 1 \\ x_{1,B} & x_{2,B} & 1 \\ x_{1,C} & x_{2,C} & 1 \end{vmatrix} \qquad (7)$$

A search algorithm is needed to associate the field points with the surrounding Delaunay cells. Inside a triangle cell the sum of the area ratio coefficients yields $\sum_{i=1}^{3} e_i = 1$. A range restriction $e_i \in [0,1]$ for $i = 1, 2, 3$ of the area ratio coefficients can be used to determine if a field point lies inside a cell. Either the displacement field of the Delaunay cells can be interpolated for the point P as follows

$$\mathbf{u}_P = e_1 \cdot \mathbf{u}_A + e_2 \cdot \mathbf{u}_B + e_3 \cdot \mathbf{u}_C \qquad (8)$$

or the new point positions of the deformed Delaunay graph can be used to evaluate the new location of a field point:

$$\mathbf{x}_{P,new} = e_1 \cdot \mathbf{x}_{A,new} + e_2 \cdot \mathbf{x}_{B,new} + e_3 \cdot \mathbf{x}_{C,new} . \qquad (9)$$

An illustration of the linear mapping approach showing an undeformed Delaunay cell and a new deformed Delaunay cell can be seen in figure 3. The extension of this algorithm to 3D can be easily achieved. In 3D a tetrahedralization of the boundary point set needs to be constructed. Barycentric coordinates can be evaluated for tetrahedra cells likewise.

3 RESULTS

The capability of the new mesh deformation approach is investigated by analysing the mesh quality for the rotation of an airfoil. Furthermore, we demonstrate the applicability of the developed approach for a mode shape deformation applied to an aeroelastic relevant 3D test case.

3.1 Airfoil rotation test case: Viscous mesh

In this section the quality of the deformation algorithms RBF and DGM is analysed and compared to the developed reduced RBF deformation algorithm. For viscous calculations a high resolution of the boundary layer is necessary. For accuracy reasons it is desired that the orthogonality of the structured boundary layer is sustained as far as possible. In order to investigate this requirement the rotation of a NACA0015 airfoil C-grid is analysed. This mesh is shown in figure 4 and consists of 39666 points, 39300 cells, 566 far field boundary points and 166 wall boundary points.

The mesh quality is measured in terms of the skewness of the cells. A perfect orthogonal cell has a skewness of zero. The mean skewness of the present mesh is 0.071. This value
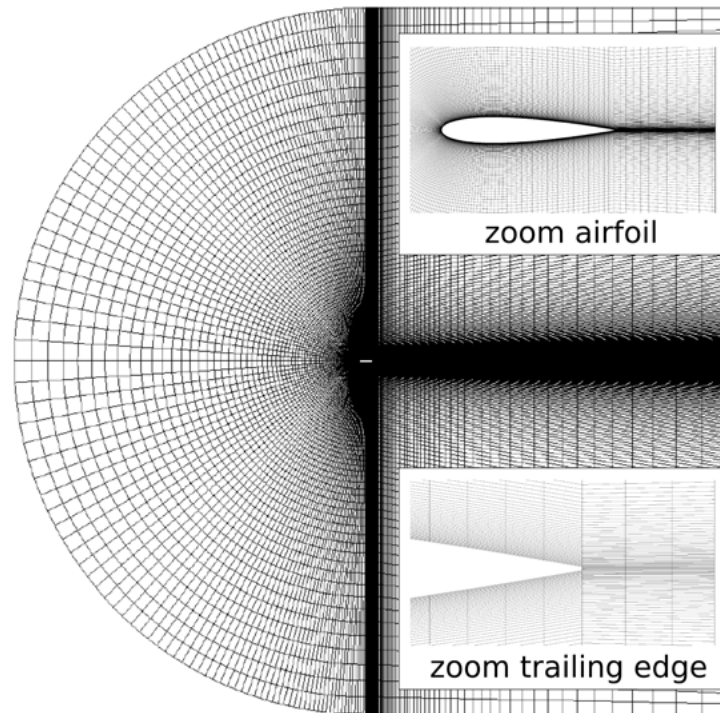
Figure 4: Airfoil NACA0015 test case: Undeformed original mesh.

is obtained by integrating all cell skewnesses over the entire mesh domain and dividing the value by the total mesh area. The largest skewness of the undeformed mesh is 0.175.

Using the original RBF and DGM approaches from literature as well as the newly developed reduced RBF deformation approach, the rotation of the airfoil is investigated. For simplicity no variation on the type of radial basis functions is analysed. We use the global thin plate spline, which performed best of the global radial basis functions studied in [6]. We focus on the analyses of a large reduction of source points used for the RBF step. The rotation of 15° is computed in three equal steps.

The resulting deformed meshes of the pure DGM deformation and the reduced RBF deformation are shown in figure 5. The DGM algorithm alone is not capable of sustaining orthogonality at the interface as can be seen in figure 5(a). Although the developed reduced RBF deformation makes use of a massive reduction in RBF source points a fairly good orthogonal behaviour can be drawn from figure 5(b). In total only 10 source points are used for the RBF deformation step. This is a source point reduction of 98.63%.

A comparison of all analysed algorithms is shown for the average and maximum skewness in figure 6. The DGM approach produces a much better average skewness, but has a drawback in the maximum skewness. The RBF approach generates the lowest maximum skewness for each deformation step. The comparison of all studied approaches shows that the combination of both approaches with a large reduction of RBF source points leads to a competitive approach for this test case. Even for a reduction to a low number of source
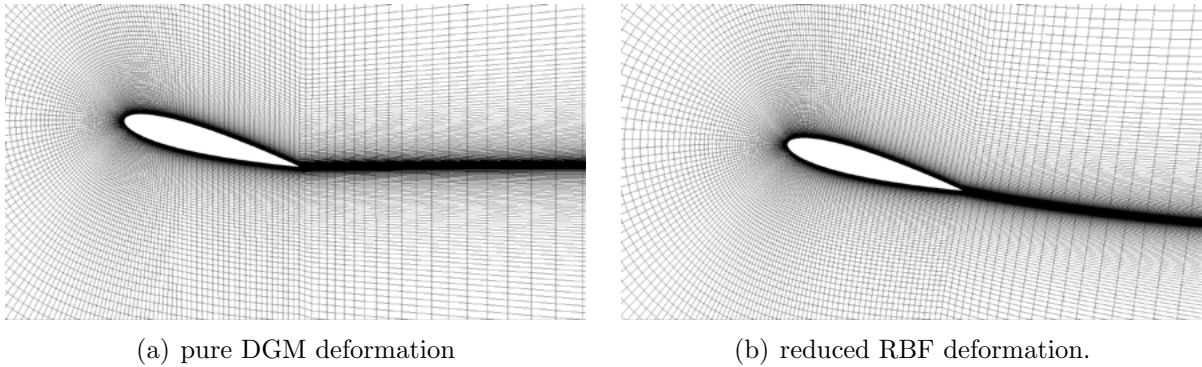
| (a) pure DGM deformation | (b) reduced RBF deformation. |

Figure 5: deformed Airfoil due to 15° rotation (parameters of reduced RBF deformation: 1 RBF and 1 Delaunay step; 4 RBF source points of the airfoil; 6 RBF source points of the farfield).

points, the quality of the deformed mesh lies in the vicinity of the pure RBF approach.

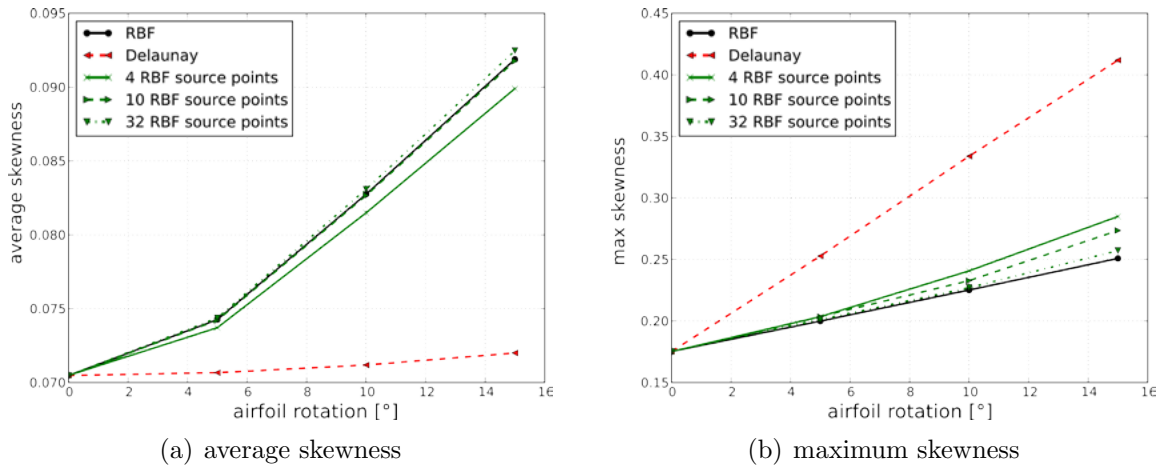| (a) average skewness | (b) maximum skewness |

Figure 6: Mesh quality for the airfoil rotation test case (reduced RBF approach: Reduction of source points is only used for the rotating boundary; 6 far field points are used for the RBF deformation step).

3.2 Wing mode shape deformation test case: Euler mesh

In this section the AGARD 445.6 wing is deformed in order to demonstrate the applicability of the developed deformation algorithm to three dimensions. The test case consists of an unstructured euler mesh with 334861 cells and 64943 points. The number of fixed boundary points is 923 and the number of moving boundary points is 16285. The mean aspect ratio of the undeformed mesh is 1.546 and the maximum aspect ratio is 7.223. The aspect ratio of a perfect tetrahedra is exactly one.

The first mode shape is used an prescribed as a large deformation field. Parts of the final deformed volume mesh are shown in figure 7. In figure 7(a) the undeformed surface mesh and the deformed surface mesh are coloured in red and green, respectively. A close view of

the deformed volume mesh at the trailing edge of the wing tip can be seen in figure 7(b). For this large deformation a reduction of 98.2% wing surface source points is used. The deformation is subdivided in one reduced RBF step and three DGM reconstruction steps. The mean aspect ratio of the deformed mesh is 1.548 and the maximum aspect ratio is 15.609. This is still a fairly good value considering the large deformation, especially for a total of only four mesh deformation steps, one reduced RBF step and three DGM reconstruction steps.
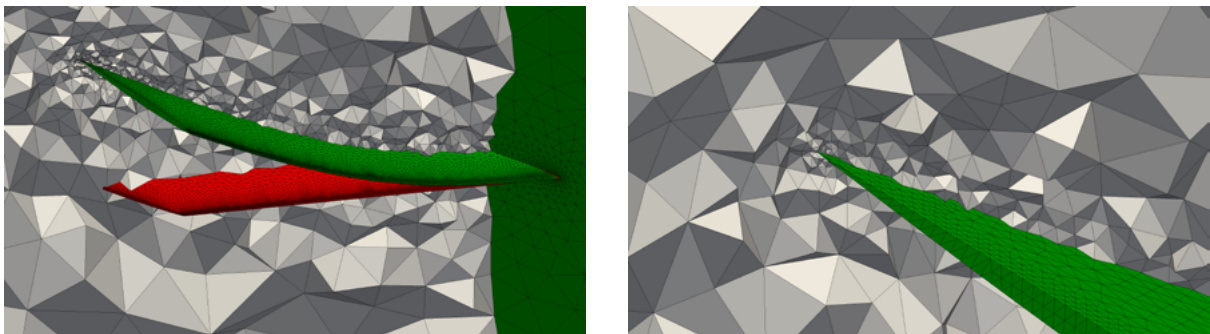
(a) Deformed volume mesh (grey); Deformed surface mesh (green); Undeformed surface mesh (red).

(b) Close view of the deformed wing tip near the trailing edge.

Figure 7: Wing test case: Deformed wing mesh using 293 of 16285 boundary points (1 reduced RBF step, 3 Delaunay reconstruction steps).

4   CONCLUSIONS

In this paper a new mesh deformation algorithm is developed by combining two well proven deformation algorithms in a three-step approach. The first pre-processing step is needed to realize a reduction of deformation source points in order to achieve a small limited amount of source points for the following radial basis function deformation step. In order to keep an overall point based scheme no surface connectivity is taken into account. A surface point reduction technique based on a k-d tree is presented. In the second step the classic radial basis function (RBF) interpolation is used to propagate the reduced deformation field. In a last post-processing step an exact surface reconstruction is achieved using an efficient Delaunay graph mapping (DGM) approach.

The new algorithm is analysed and compared with the classic RBF algorithm and the DGM algorithm for a 2D viscous mesh. The new algorithm outperforms the DGM approach concerning sustainment of cell orthogonality. It is shown that the results compared to the classic RBF algorithm are almost as good, even if a large reduction of source points is used. Furthermore, the applicability of the new algorithm to 3D was shown with an aeroelastic relevant test case.

Future research will focus on the analyses and comparison to other methods for more relevant test cases and on applying this approach to a fluid-structure interaction analysis.

REFERENCES

[1] Batina, J.T. Unsteady Euler algorithm with unstructured dynamic mesh for complex-aircraft aerodynamic analysis. *AIAA Journal* (1989) **29**(3):327-333.

[2] Farhat, C., Degand, C., Koobus, B. and Lesoinne, M. Torsional springs for two-dimensional dynamic unstructured fluid meshes. *Comput. Methods Appl. Mech. Engrg.* (1998) **163**:231-245.

[3] Lynch, D.R. and ONeill, K. *Elastic grid deformation for moving boundary problems in two space dimensions.* S.Y. Wang, C.V. Alonso, C.A. Brebbia, W.G. Gray, G.F. Pinder (Eds.) Finite Elements in Water Resources, Vol. III. (1980).

[4] Stein, K., Tezduyar, T.E. and Benney R. Automatic mesh update with the solid-extension mesh moving technique. *Comp. Meth. Appl. Mech. Engrg.* (2004) **193**:2019-2032.

[5] Beckert, M.A. and Wendland, H. Multivariate interpolation for fluidstructure-interaction problems using radial basis functions. *Aerospace Science and Technology* (2001) **5**:125-134.

[6] de Boer, A., van der Schoot, M.S. and Bijl, H. Mesh deformation based on radial basis function interpolation. *Computers and Structures* (2007) **85**:784-795.

[7] Michler, A.K. Aircraft control surface deflection using RBF-based mesh deformation. *Int. J. Numer. Meth. Engng.* (2011) **88**:986-1007.

[8] Rendall, T.C.S. and Allen, C.B. Efficient mesh motion using radial basis functions with data reduction algorithms. *Journal of Computational Physics* (2009) **228** (17):6231-6249.

[9] Wendland, H. Piecewise polynomial, positive definite and compactly supported radial basis functions of minimal degree. *Adv. Comput. Math.* (1995) **4**:389-396.

[10] Liu, X., Qin, N. and Xia, H. Fast dynamic grid deformation based on Delaunay graph mapping. *Journal of Computational Physics* (2006) **211**:405-423.

[11] Wendland H. Konstruktion und Untersuchung radialer Basisfunktionen mit kompaktem Trger. *Tech. Rep.* (1996).

[12] Barber, C.B., Dobkin, D.P. and Huhdanpaa, H.T. The Quickhull algorithm for convex hulls. *ACM Trans. on Mathematical Software* (1996) **22**(4):469-483, http://www.qhull.org.

[13] Kitware, Inc. *VTK User's Guide.* Kitware, Inc. 11th Edition (2010).